CHAPTER IV
RESULTS AND DISCUSSION

In this study, Single-Walled Carbon Nanotubes (SWNTs) were produced by CoMoCAT@ process in which cobalt nitrate and ammonium heptamolybdate act as precursor over a silica support. However, the properties of SWNTs are hindered from the impurities derived from the production processing step. From, the proposed growth mechanism of SWNTs on the catalyst (Resasco *et al.*, 2002), the SWNTs are grown vertically forward on the metal catalyst. Therefore, the purified as-prepared SWNTs can be achieved by removal of the metal catalyst. (Chuaybumrung, 2005). In this study, the SWNT purification comprised four sequential steps. Oxidative pretreatment was first employed to eliminate the amorphous or encapsulated disordered carbon layer, permitting the increasing removal of the catalysts with acid leaching (Chiang *et al.*, 2001). The optimum oxidation temperature was attained by using temperature gravimetric analysis (TGA). Then, hydrochloric acid was used to dissolve the metal catalyst (Bougrine *et al.*, 1999) leading to the detachment of SWNTs from the silica support. The concentration, time, and dissolution temperature were investigated. The silica of the SWNTs samples was further dissolved using sodium hydroxide. Finally, froth flotation was applied to separate the SWNTs from the silica support using two types of surfactants: sodium dodecyl benzene sulfonate (SDBS), and also alcohol etoxylate-surfonic L24-7 (Nonionic).

4.1 Production of Single-Walled Carbon Nanotubes (SWNTs)

The SWNTs synthesis was conducted by using the disproportionnation of carbon monoxide (CO) over a cobalt-molybdenum catalyst, which is designated by CoMoCAT. The total metallic loading in the catalyst was 6 wt %, while the Co:Mo molar ratio was 1:3. Prior to the production of SWNTs by the CO dissproportionation, the catalyst was pretreated by heating to 500°C under a flow of hydrogen (H_2), and further heated to 850°C in the presence of helium (He). This reduction/heating pretreatment is essential to obtain a high selectivity of SWNTs; however, the SWNTs still contained the spent catalyst and the silica support.

To characterize the SWNTs, a combination of scanning electron microscope (SEM), laser Raman spectroscopy, and temperature programmed oxidation (TPO) were used. Laser Raman spectroscopy is a particularly powerful technique for characterizing the structure of carbon nanotubes and providing information about purity, distribution of tube diameters, and electronic properties. The Raman spectra of SWNTs, as shown in Figure 4.1, exhibits several important bands: a) Radial A_{1g} Breathing Mode (RBM), the series of the band in a range of 150-400 cm^{-1}, whose position can be used to estimate the nanotube diameter (Rao, *et al.*, 1997); b) the so-called D-band is around 1350 cm^{-1}, which relates to defects or disordered carbon and the presence of carbon nanoparticles and amorphous carbon; c) the tangle mode G-band appearing in the 1400-1700 cm^{-1} region, which relates to the Raman-allowed phonon mode E_{2g}, and involves out-of-phase intralayer displacement in the graphene structure. It provides information about the electronics properties for distinguishing between metallic and semiconducting single-walled carbon nanotubes.

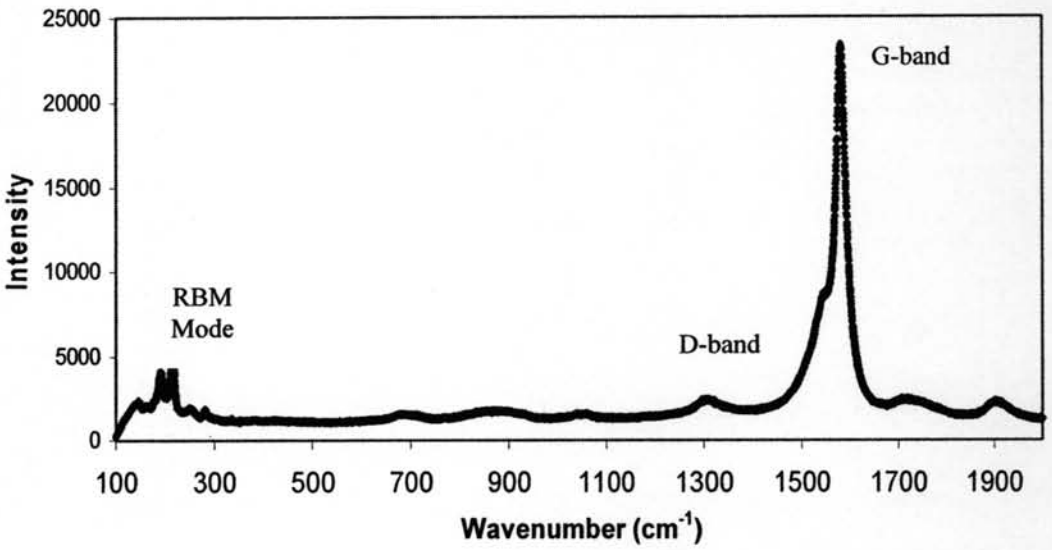

Figure 4.1 Raman spectra of SWNTs produced by the CO disporportionnation over 1:3 CoMo loaded on silica at 850°C.

In addition, the D-band to G-band (D/G) intensity ratio provides a relative amount of disordered carbon to graphite-like carbon. Typically, if the relative intensity ratio (D/G) is low, this indicates that the formation of disordered carbon is less than

graphic-like carbon. Hence, it means that the carbon mostly consists of graphite-like forms as SWNTs, MWNTs and nanofiber. In contrast, if the relative intensity ratio (D/G) is high, the implication is that the sample mainly contains mostly disordered carbon form.

The TPO was also employed to confirm the carbonaceous types depositing on the spent catalyst. Carbon with different morphologies is oxidized at different temperatures. Therefore, examining the oxidation temperature helps to identify the types of carbon products. Figure 4.2 shows the TPO curve of as-prepared SWNT sample. It has been reported that the oxidation of amorphous carbon on this type of catalyst under the particular conditions used in this work has a range of 300 to 400°C, while SWNTs and MWNTs have shown peaks around 495-530°C and 600-700°C, respectively (Kitiyanan *et al.*, 2000). The quantity of carbonaceous species deposits on the catalyst, which was calculated by fitting the entire profiles with the Gaussian-Iorenzian mixture.Table 4.1 shows the compositions of all carbons in the as-prepared SWNTs as compared to commercial of SWNT and commercial MWNT samples. According to both the Raman and the TPO results, most of the carbon products in the as-prepared SWNT sample was found in SWNT form. The total carbon yield was about 2.55 wt.%.

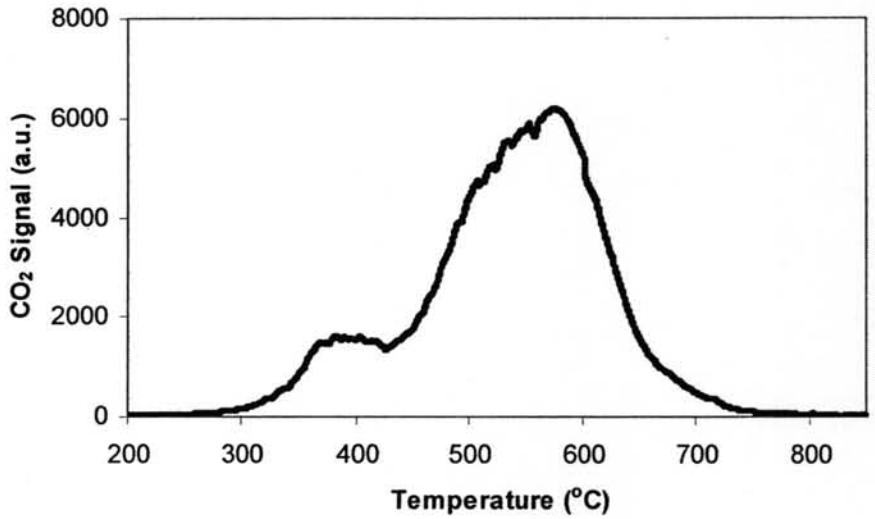

Figure 4.2 Temperature Programmed Oxidation (TPO) profile of the SWNT sample synthesized over in Co:Mo/SiO_2 catalyst of the decomposition of CO at 30 min

Table 4.1 Types of carbonaceous species present in the as-prepared SWNT sample compared to commercial MWNT and SWNT samples

Type of SWNTs	Selectivity (%)[(a)]			Total carbon[(a)]
	Amorphous	SWNTs	MWNTs	Yield (%)
As-prepard SWNTs	18.78	47.32	33.88	2.55
Commercial SWNTs	8.91	60.87	30.30	65.43
Commercial MWNTs	1.19	6.158	92.64	87.17

[a] Yield is defined as the percent weight of carbon deposited per total catalyst weight, Similarly, selectivity is defined as the percent of carbon products deposited on the catalyst in the form of SWNTs.

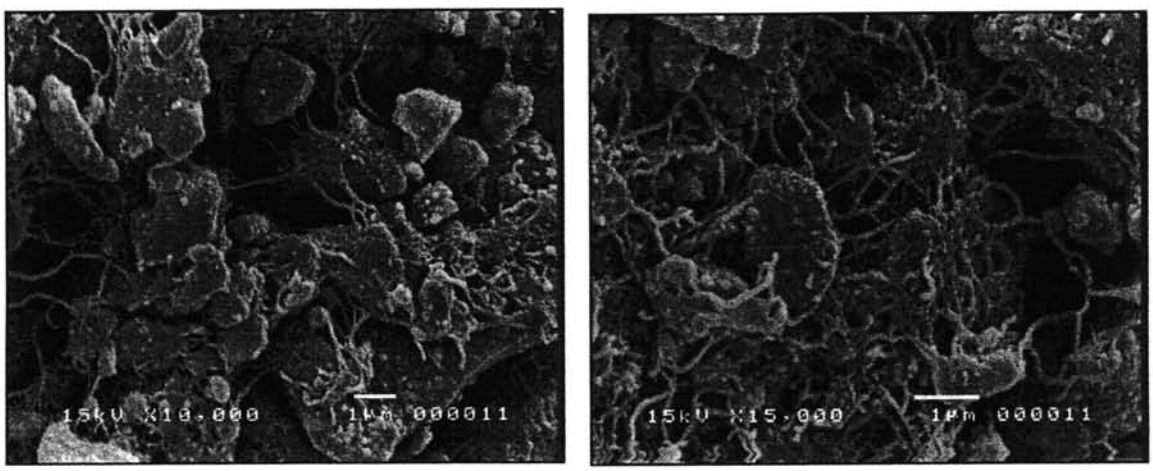

(a) (b)

Figure 4.3 Scanning electron microscope (SEM) images of as-prepared SWNTs at (a) 10,000 x, (b) 15,000 x.

The images of the scanning electron microscope of the as-prepared SNWT sample are shown in Figure 4.3. The as-prepared SWNTs contained obviously the silica support in their structure, and also exhibited the presence of the typical rope-like bundles which are similar to the structures grown by the other methods (Satishkumar *et al.,* 1998). Besides, a thin layer of amorphous carbon was found to cover the SWNTs bundles.

4.2 Oxidative Pretreatment

According to the synthesis procedure, the metals are typically present as nanoparticles with carbon coating which varies from disorder carbon layers to graphitic shells, leading to the prevention of the acid solution efficiently dissolving the metal particles from the carbonaceous species. Chiang. *et al.,* (2001) found that the low temperature oxidation can remove effectively the disordered carbon layer, which permits removal of this metal with the acid solution. In this study, Temperature Gravimetric Analysis (TGA) was employ to verify the transformation of the metal to metal oxides

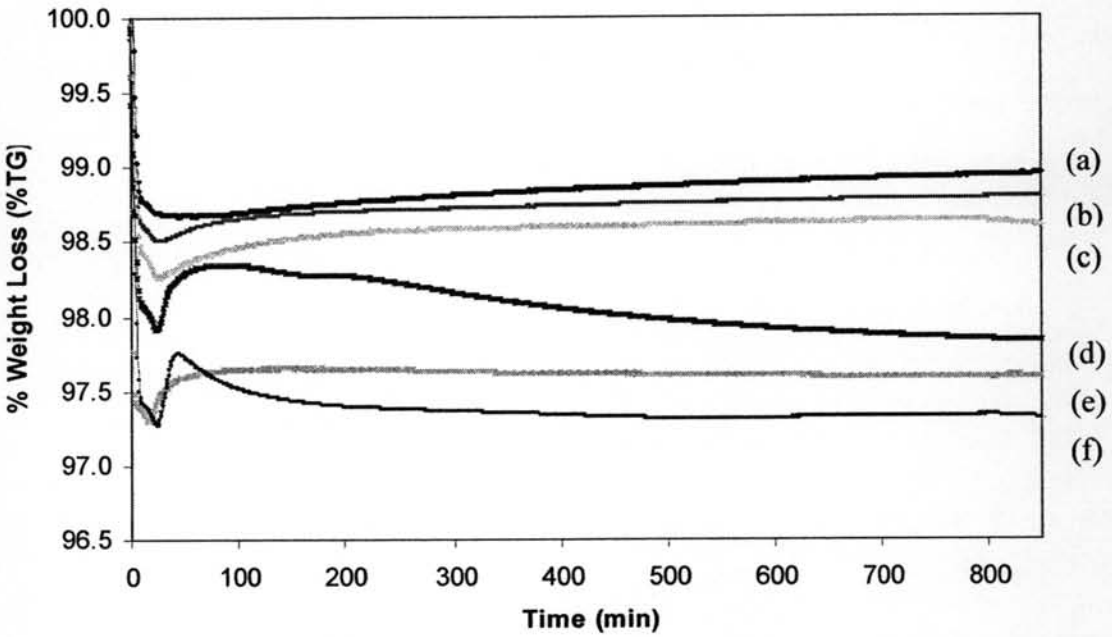

Figure 4.4 Temperature gravity analysis (TGA) investigating pretreatment at various temperatures in with presence of 5% O_2 balanced in He: (a) 200°C, (b) 225°C, (c) 250°C, (d) 300°C, (e) 350°C, and (f) 400°C.

The pristine SWNTs are subjected to the oxidation in O_2 environments as a function of time at different temperatures as shown by the TGA profile in Figure 4.4. At first, the weight dramatically decreased as a consequence of the water and amorphous carbon loss. The weight gains were observed during the second period of heating for each oxidation temperature as a result of the oxidation of the metal

particles, similar to the attribution of oxidation of SWNTs obtained from HiPco (Chiang. *et al.*, 2001). This phenomenon was to breach the carbon shell and transform the metal particles to an oxide and/or hydroxide. However, the actual form of the metallic catalyst of Co and Mo are identified by using XPS technique, as shown in Figure 4.5.

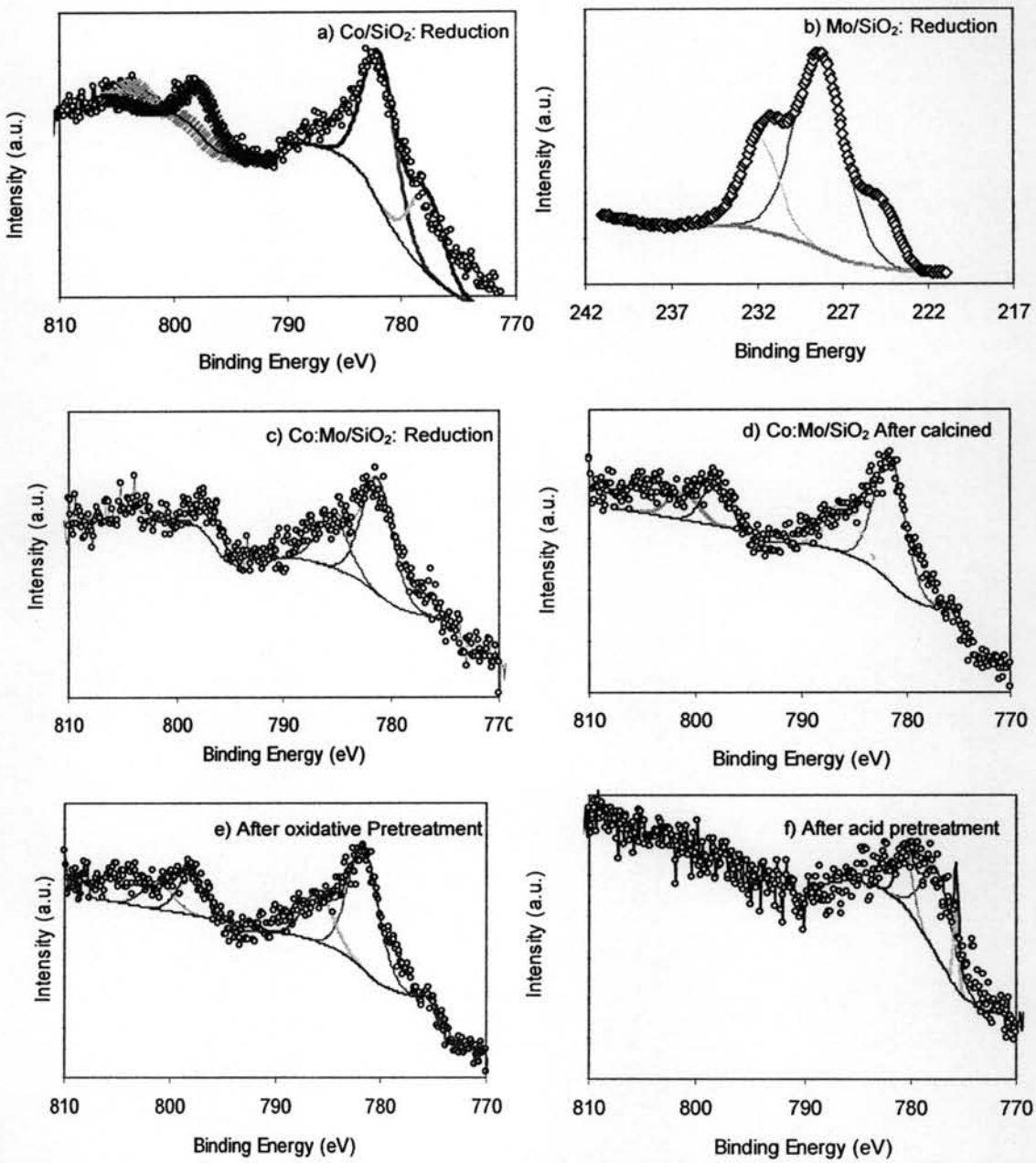

Figure 4.5 XPS results showing Co 2p and Mo 3d spectra of a) Co/SiO_2: Reduction, b) Mo/SiO_2: Reduction, c) $Co:Mo/SiO_2$: Reduction, d) $Co:Mo/SiO_2$: After calcined, e) after oxidative pretreatment, and f) after acid pretreatment.

Table 4.2 XPS of Binding Energies (BEs) of Co 2p and Mo 3d spectra of sample

Samples	Binding Energy (eV)			
	C1s	O 1s	Mo $3d_{5/2}$	Co $2p_{3/2}$
Reduced Co	284.8	533.56	-	781.68
Reduced Mo	284.8	528.88	228.19	-
Reduced Co:Mo/SiO_2	284.8	533.34	232.2	781.92
Co:Mo/SiO_2				
. after calcinations	284.8	533.88	232.52	781.89
- after oxidation	284.8	531.36	232.52	781.89
- after acid pretreatment	284.8	531.36	232.52	780.27

The selectivity of the Co-Mo catalysts toward SWNTs strongly depends on the stabilization of the Co species in a nonmetallic state before exposure to CO, resulting from the Co-Mo interaction, which is a function of the Co/Mo ratio and has different forms during the stages of the catalyst life. From the detailed characterization conducted over the catalyst series, Alvarez, *et al* (2002) concluded that, after calcination, Mo is in the form of well-dispersed molybdenum (6+) oxide, while Co is either interacting with Mo in a superficial cobalt molydate-like structure (at low Co/Mo ratios) or as non-interacting Co_3O_4 phase (at high Co/Mo ratios). After a subsequent treatment in hydrogen, the non-interacting phase is reduced to metallic Co, whereas Co in the molybdate-like species remains as well-dispersed Co2+ ions. During the production of SWNTs under the pure CO enviroment, the molybdenum oxide species is converted into molybdenum carbide. This conversion disrupts the interaction between Co and Mo and results in the release of metallic Co in the form of extremely small clusters, which are responsible for the production of SWNTs (Alvarez, *et al.*, 2002). In contrast, large Co clusters formed from the non-interacting Co phase produce the nonselective forms of carbon (MWNTs, nanofibers filament and graphite).

Table 4.2 summarizes the binding energies of all forms of Co and Mo for confirming the chemical stage of both metal forms before and after the reaction and treatment. For the reduced Co/SiO_2 and reduced Mo/SiO_2 samples, the peak position is close to Co $2p_{3/2}$ = 780.5 eV (Herrera, *et al.,* 2004) and Mo $3d_{5/2}$ = 227 eV (Reference for Line Energy) for the Co and Mo, respectively. After the reduction of the

Co:Mo/SiO_2 samples, the peak position of Co and Mo indicated the synergism of the $CoMoO_4$ structure on the surfaces, corresponding to the Co $2p_{3/2}$ = 781 eV and Mo $3d_{5/2}$ = 232.6 eV (Parola,. *et al.*, 2002). During the synthesis step of SWNTs using CO as a carbon source, the molybdenum oxide species is converted into molybdenum carbide, resulting in the release of metallic Co in the form of extremely small clusters. The structure of any transition metal is similar to the investigation of structure using EXAFS data (Alvarez, *et al.*, 2001). After the oxidative pretreatment step, the metallic Co was converted into Co_3O_4 as indicated by the peak shift of Co $2p_{3/2}$ = 781.89 eV. The cobalt compounds have different Co $2p_{3/2}$ binding energies depending on the different oxidic environments. The Co $2p_{3/2}$ of mixed oxide Co_3O_4 has two peak positions, one at low energy corresponding to the Co^{2+} species and the other at a higher value corresponding to the Co^{3+} oxidation state species, whereas molybdenum carbide was converted into MoO_3 (Mo $3d_{5/2}$ = 232.52 eV). The results are in good agreement with XPS data (Herreara, *et al.*, 2001). In confirming the structures of Co and Mo using XPS results, it is obvious that the oxidative pretreatment results in thermal expansion due to the fact that the densities of Co metallic and molybdenum carbide (Mo_2C) particles significantly increase to Co_3O_4 and MoO_3 from 8.9 to 6.07 g/cm^3 and from 8.9 to 4.7 g/cm^3 (Perry's Chemical Engineers), respectively. This thermal expansion leads to breaking the encapsulated carbon shell.

Table 4.3 Weight loss and total carbon content after the oxidative pretreatment at different temperatures.

Oxidative Pretreatment Temperature (°C)	% Total Carbon	% Weight Loss
0	2.55	0.00
200	2.38	6.80
225	2.37	7.16
250	2.35	7.87
300	2.19	14.25
350	1.63	34.49
400	1.65	35.29

Table 4.3 and Figure 4.6 show the weight loss and the total carbon content after the oxidative pretreatment at different temperatures. As the oxidation temperatures increased, the total carbon content decreased whereas the weight loss increased.

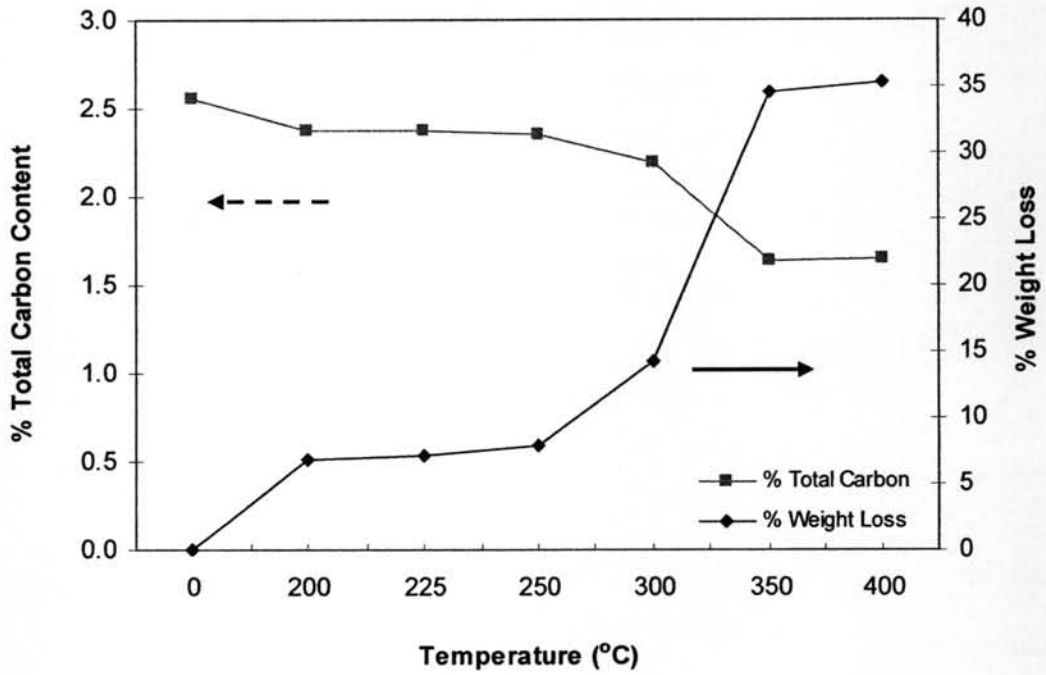

Figure 4.6 Effect of oxidation temperature on weight loss and total carbon content after the oxidative pretreatment of as-prepared SWNT sample.

Figure 4.7 shows the changes of all carbon forms during the oxidative pretreatment at different temperatures of the as-prepared SWNT sample. Interestingly, the SWNTs remained unchanged in the studied temperature range of 200-400°C whereas the MWNTs started to decreased with increases temperature from 250 to 400°C. For the amorphous carbon, it decreased with increasing temperature in the range of 200-250°C. Beyond 250°C, the amorphous carbon increased substantially with increasing temperature up to 400°C. The results suggest that the SWNTs are thermally stable up to 400°C while the SWNTs are less thermally stable only up to 250 °C. The increase in the amorphous carbon beyond 250°C can be explained in that the MWNTs are converted into amorphous carbon. From the TPO and Raman results, the oxidation temperature of 250°C was selected for further investigation.

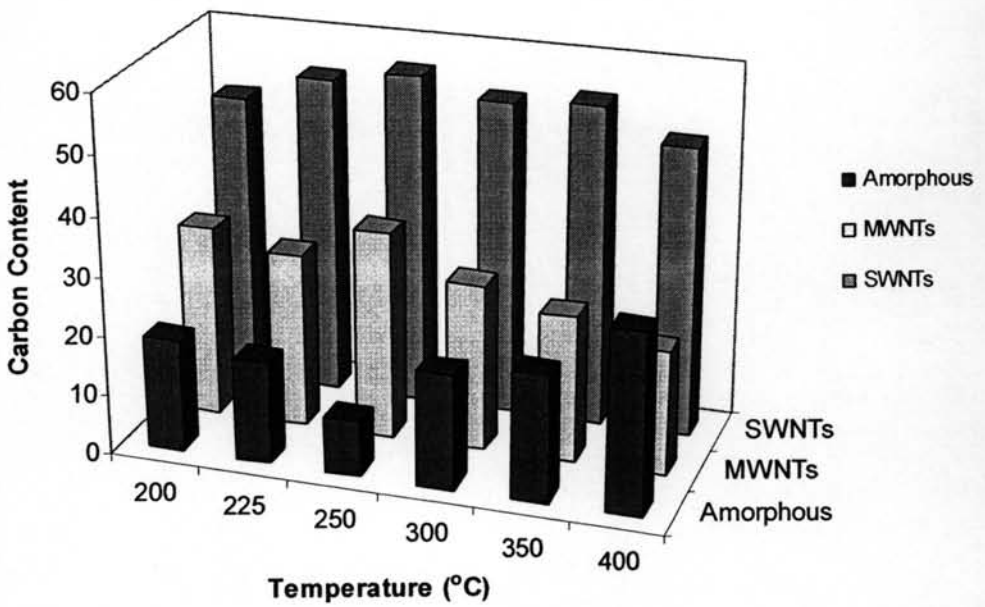

Figure 4.7 % Carbon contents of all carbonaceous species after the oxidative pretreatment with different temperatures.

4.3 Acid Treatment Results

The oxidative pretreatment was carried out at an optimum temperature of 250°C for the as-prepared SWNT sample. This treated sample was then taken for the acid treatment experiments. HCl was selected to dissolve the oxidized catalyst metals (Co and Mo).

Table 4.4 Percent catalyst removal with and without oxidative pretreatment

Concentration of HCl (M)	% Removal			
	With the oxidative pretreatment		Non-Oxidative Pretreatment	
	Co (ppm)	Mo (ppm)	Co (ppm)	Mo (ppm)
1	98.2	73.0	7.6	6.7
5	99.8	86.2	11.8	9.2
12	99.8	90.0	12.0	9.4

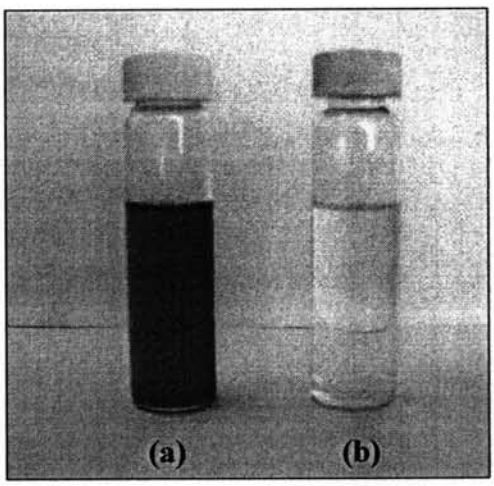

Figure 4.8 Comparative colors of HCl solution after digestion of a) the oxidative pretreatment samples, and b) the samples without oxidative pretreatment.

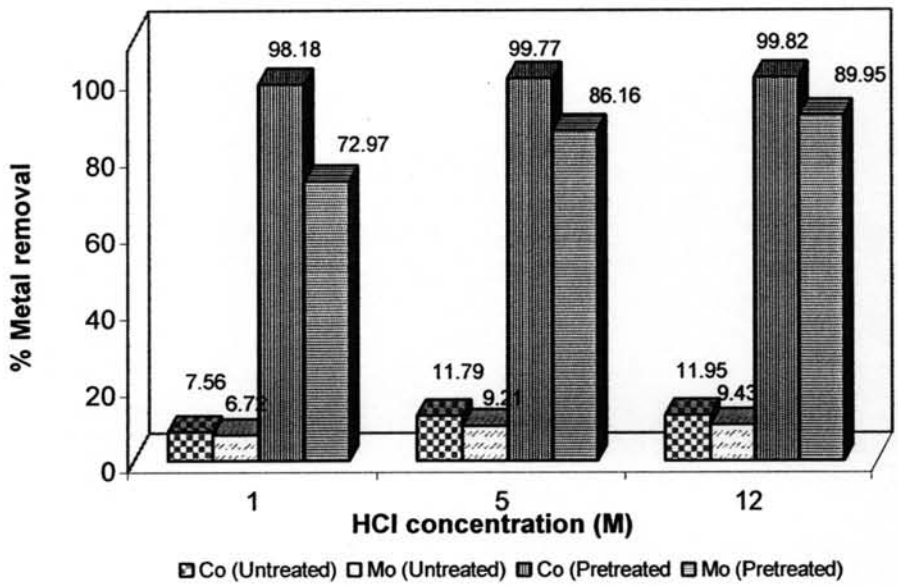

Figure 4.9 Effect of HCl concentration on catalyst removal with and without oxidative pretreatment at 80°C for 12 h.

Table 4.4 shows the catalyst removal efficiency of the oxidized SWNT sample as compared to that of the as-prepared SWNT sample. As seen in Table 4.4, the oxidative pretreatment step plays a significant role in the enhancement of catalyst

removal. The results can be explained in that during the oxidative pretreatment, the change of the metallic Co and Mo to the metal oxides results in the volumetric expansion, leading to some of the carbon layer covering the catalysts to be cracked. Consequently, the higher the exposure surface of the catalysts, the higher the catalyst removal. Figure 4.8 shows the color change when the SWNT was oxidized.

Table 4.5 Removal of Co and Mo of the oxidized SWNT sample at different HCl concentrations, 80°C, and 12 h

HCl Concentration (M)	% Removal	
	Co	Mo
0.5	90.0	55.2
1.0	98.2	73.0
5.0	97.9	86.2
8.0	99.6	89.6
12.0	99.8	89.8

Table 4.5 and Figure 4.10 show the effect of HCl concentration on removal of Co and Mo of the as-prepared SWNT sample treated with air oxidation. For any given, the removal increased and reached a maximum level with increasing HCl concentration. Interestingly, the Co removal was significantly higher than Mo as result of Co is less stable than Mo. Moreover, the bundle of SWNTs might have intercalated on the Mo catalyst, which prohibited acid leaching; resulting in the removal of Mo not approaching a high level (Resasco. D.E. *et al.*, 2002). From the results, 5 M of HCl was considered as an optimum condition which was selected for further investigation.

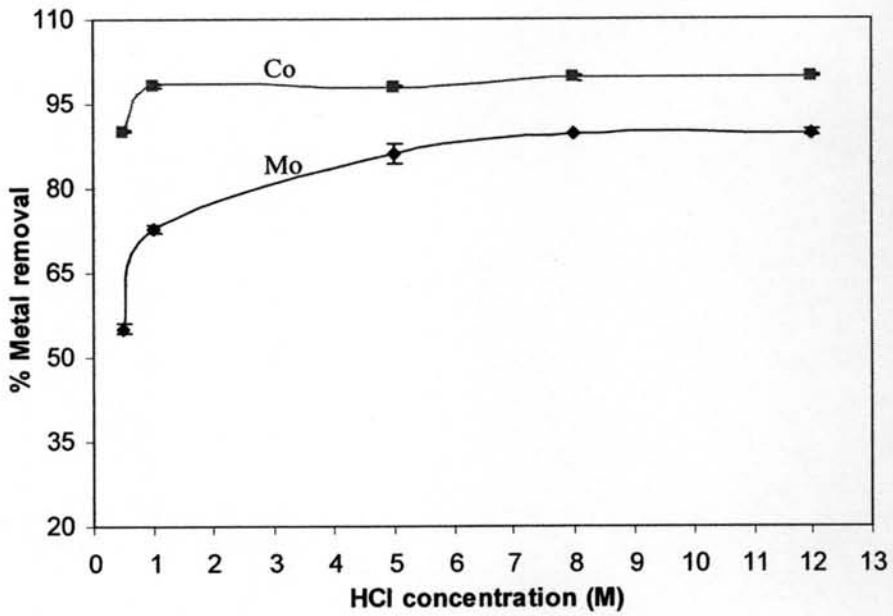

Figure 4.10 Removal of Co and Mo metal catalyst of the oxidized SWNT sample at different HCl concentrations, 80°C, and 12 h.

Table 4.6 and Figure 4.11 show the effect of sonication time on the removal of Co and Mo of the oxidized SWNT sample at 5 M HCl and 80°C. When the sonication increased, the removal of both Co and Mo increased and reached maximum values around 5 h. Therefore, 5 h of sonication time was selected for further experiments.

Table 4.6 Effect of sonication time on the removal Co and Mo of oxidized SWNT sample at 5 M HCl and 80°C

Time	% Removal	
(h)	Co	Mo
1	82.2	64.0
3	89.0	71.9
6	95.5	88.5
12	98.2	91.5

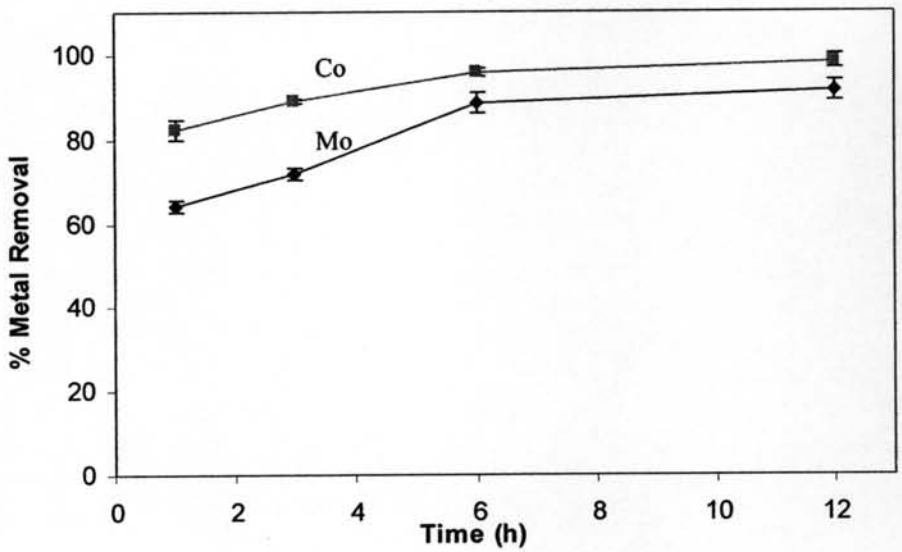

Figure 4.11 Removal of Co and Mo of the oxidized SWNT sample at different times, 5 M HCl, and 80°C.

Table 4.7 and Figure 4.12 show the effect of temperature on the removal of Co and Mo of the oxidized SWNT sample dissolved with 5 M HCl. The removal of Mo increased with increasing temperature whereas the removal of Co remained unchanged. The results can be explained that the Co removal almost reaches its maximum level. For the results, 80°C was selected as a base condition for next experiment.

Table 4.7 Removal of Co and Mo of oxidized SWNT sample at different temperatures under 5 M HCl and 5 h

Temperature	% Removal	
(h)	Co	Mo
30	93.6	62.8
40	95.1	70.3
65	94.0	84.6
80	95.1	90.0

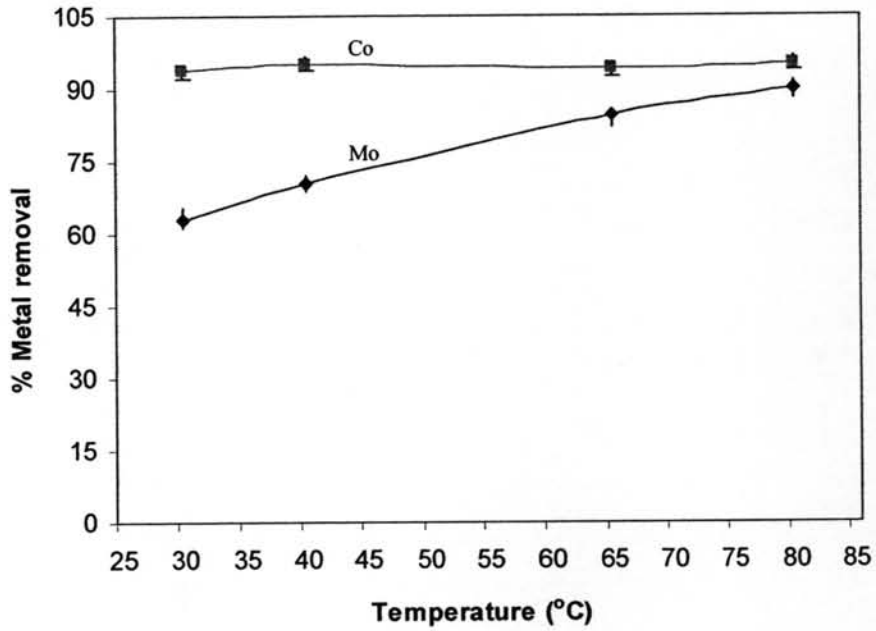

Figure 4.12 Removal Co and Mo of oxidized SWNT sample at different temperatures, 5 M, and 5 h.

Table 4.8 and Figure 4.13 show the effect of cycle number of the acid treatment on the removal of Co and Mo of the oxidized SWNT sample. As the cycle number of the acid treatment, the removal of Co and Mo increased but the effect of cycle number of the acid treatment is insignificant as also shown in Figure 4.14 in term of accumulative removal. From the results, one cycle of the acid treatment is sufficient for the removal of catalyst from SWNTs

Table 4.8 The effect of cycle number of acid treatment removal of Co and Mo oxidized SWNT sample using 5 M HCl at 80°C and 5 h

Number of cycles	% Removal of each cycle	
	Co	Mo
1	92.0	89.9
2	3.4	2.1
3	1.5	1.1
4	0.2	0.1

Table 4.8 summarizes the percent removal of Co and Mo with varying cycle numbers of acid treatment. The amount of Co and Mo metal catalyst was dramatically reduced in the first acid treatment; up to 91.96% and 89.90% for Co and Mo, respectively. For another sequential treatment cycle number, the percentage of Co and Mo removal gradually increased with increasing number of cycles; from 3.4 % to 0.24% for Co and 2.09% to 0.14% for Mo as shown in Figure 4.13.

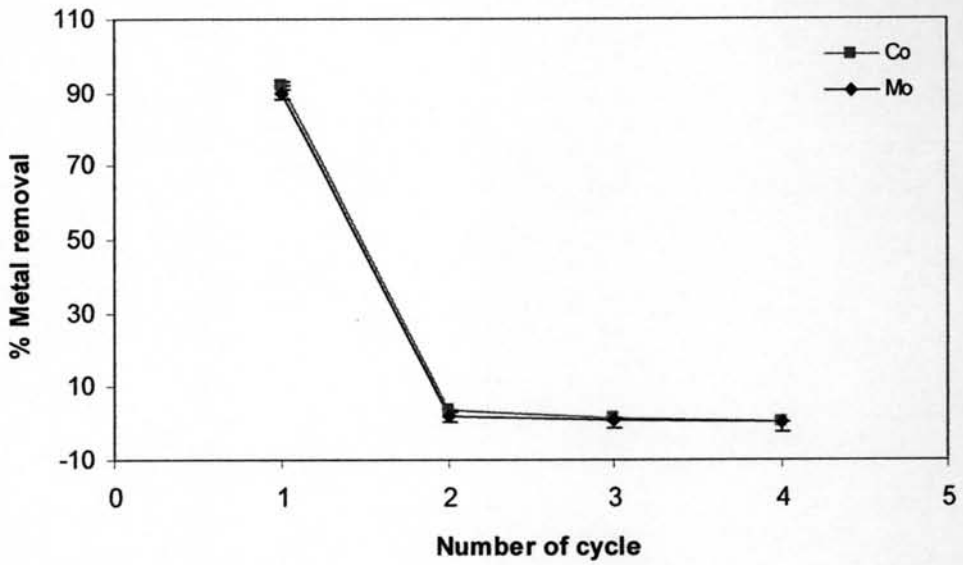

Figure 4.13 Removal of Co and Mo the oxidized SWNT sample treated with 5 M HCl at 5 h, and 80°C as a function of cycle number of acid treatment.

The accumulated of percentage removal of the metal catalysts is depicted in Figure 4.15. Even thought, in this study, they were further treated with fresh acid treatment for several cycles, the accumulated percent removal of the catalyst was not completed removal.

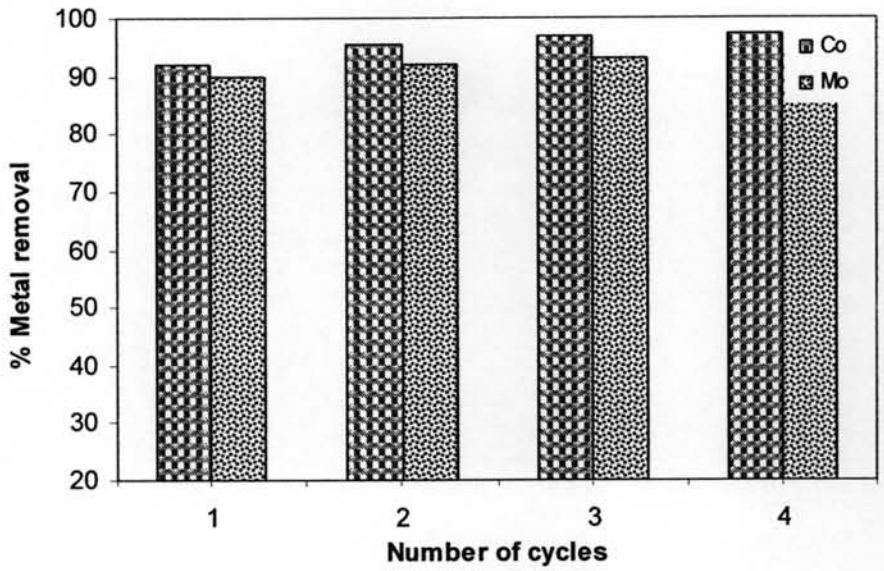

Figure 4.14 Accumulation of the percent removal of the Co and Mo metal catalyst from the as-prepared SWNT samples at 5 M HCl, 5 h and 80 °C.

4.4 Point of Zero Charge (PZC) Results

The surface charge of solid particles depends on the medium pH and the type and amount of electrolyte present. The PZC, or the point of zero charge, is defined as the pH at which the surface exhibits a net surface charge of zero. At pH values below the PZC, the substrate becomes protonated and exhibits a positive net charge on the surface. In contrast, the net surface charge turns negative at pH values above the PZC.

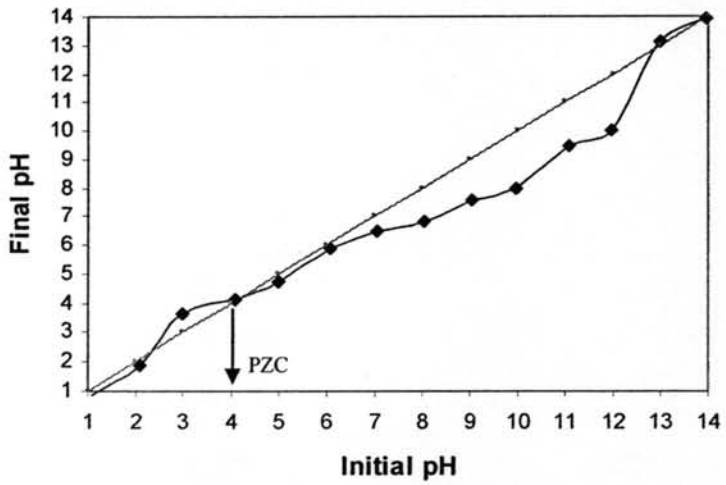

(a) Point of Zero Charge of Silica particles

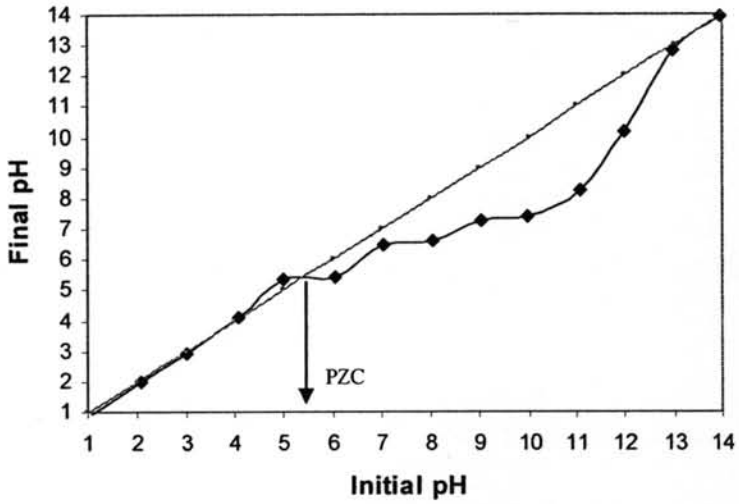

(b) Point of Zero Charge of carbon black particles

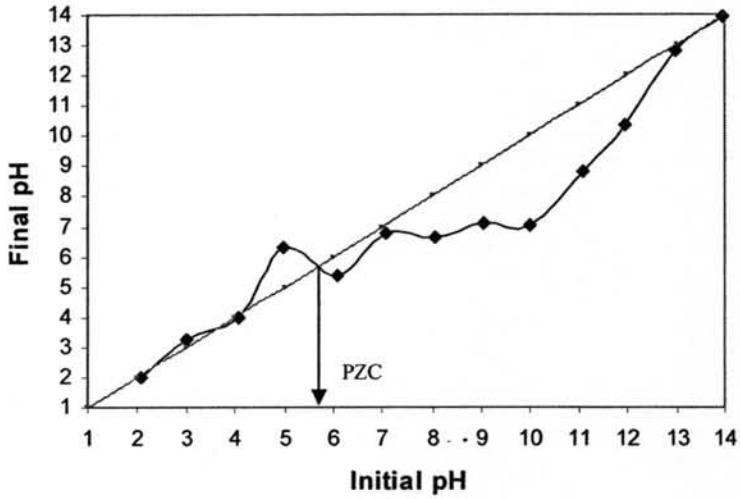

(c) Point of Zero Charge of SWNTs particles

Figure 4.15 Determination of PZC for a) silica, b) carbon black, and c) as-synthesized SWNTs.

The curves of final pH as a function of initial pH for each sample with the presence of water showed, as expected, a crossing point of the y = x line at a final pH corresponding to the PZC as illustrated in Figure 4.15. The silica sample exhibited a PZC of around 4, which is closed to PZC = 3.8 given by Parola *et al.*, (2002). While the carbon black has the PZC of 5.5; likewise, the SWNTs has the PZC of around 5.8. These investigations are in good agreement with Sun *et al.*, (2002) who previously observed the MWNT samples and found that the zeta potential of the pristine nanotubes was zero at a pH approximately 5.8.

4.5 Contact Angle Results

Normally, contact angle indicates the wettability of a substance which can infer either hydrophilic (love water) or hydrophobic (love oil) substance. The higher the contact angle become the higher the wettability or the more the hydrophobicity or the less the hydrophobicity.

Table 4.9 Contact angle value of three studied particles with pure water at 30°C

Type of particle	Contact Angle Theta (°)
Silica	15.8
Carbon Black	59.8
As-SWNTs	39.4

Table 4.9 shows the contact angles of three studied particles with pure water. Silica particles have a contact angle of around 15°, which is considered to be hydrophilic, while carbon black acts as a hydrophobic surface having its contact angle at approximately 59°. The as-prepared SWNTs have a combination of properties of the silica and the carbon black particles. Hence, the contact angle (35.4°) of the as-prepared SWNTs is between those of silica and carbon.

4.6 Critical Micelle Concentration (CMC)

Critical micelle concentration (CMC) is the concentration of a particular surfactant where micelle formation occurs, resulting in the lowest surface tension in solution because the accumulation of surfactants at the air/water interface provides lowering of the excess Gibbs free energy of the interface. Figure 4.16 shows the plot of surface tension and surfactant concentration of Sulfonic L24-7 and NaDDBS. The CMC value can be determined from the erupt point of the point. The CMC of Sulfonic L24-7 was found to be 98.1 μM which is a good agreement with previous study (Chuangcharumkit, 2004), while NaDDBS had a CMC of around 1.3 mM as quite same to the value given by Matterda *et al.*, (2003).

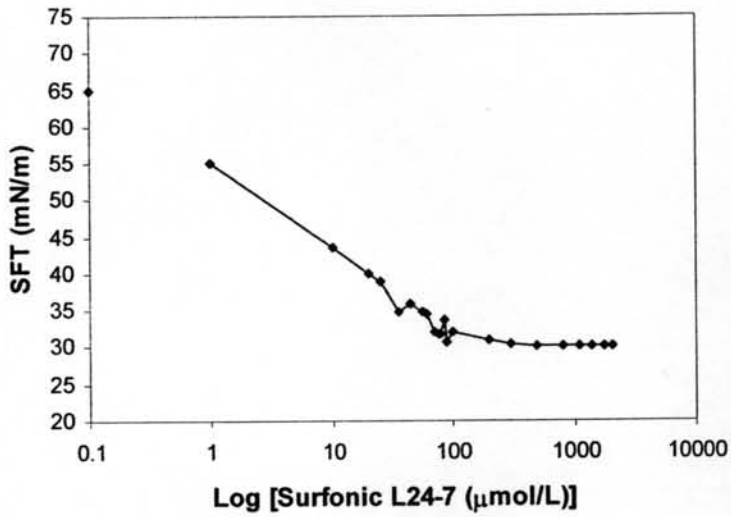

a) CMC of Sulfonic L24-7 (Nonionic surfactant)

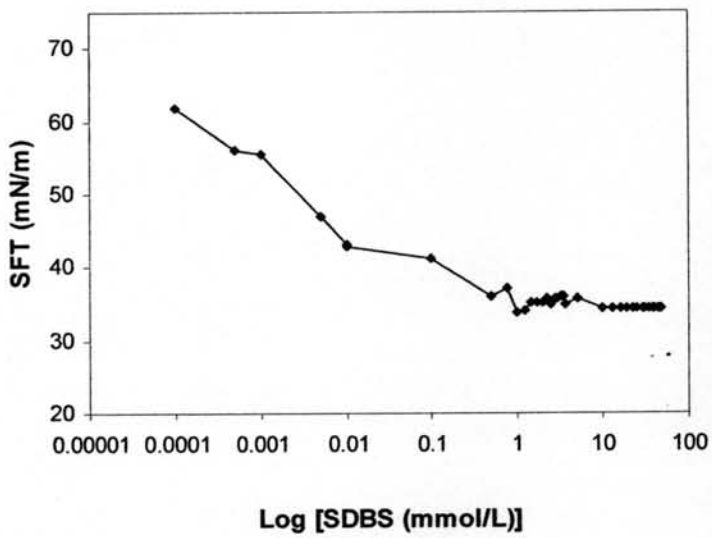

b) CMC of SDDBS (Anionic surfactant)

Figure 4.16 Surface tension as a function of surfactant concentration a) Sulfonic L24-7 (Nonionic surfactant), and b) SDDBS (Anionic surfactant) at 25°C.

4.7 Silica Dissolution Results

As described before, the as-prepared SWNT samples were first treated with the oxidative pretreatment at 250°C. The metal catalysts were converted to metal oxides, resulting in increasing the exposure of the catalyst surfaces, and partly oxidizing the amorphous, or disordered carbon at low temperature. Then, the preoxidized SWNTs sample was further treated in a 5M hydrochloric acid solution at 80°C for 5 h in order to remove the metal catalysts, which act as a bridging bone between the silica and the SWNTs.

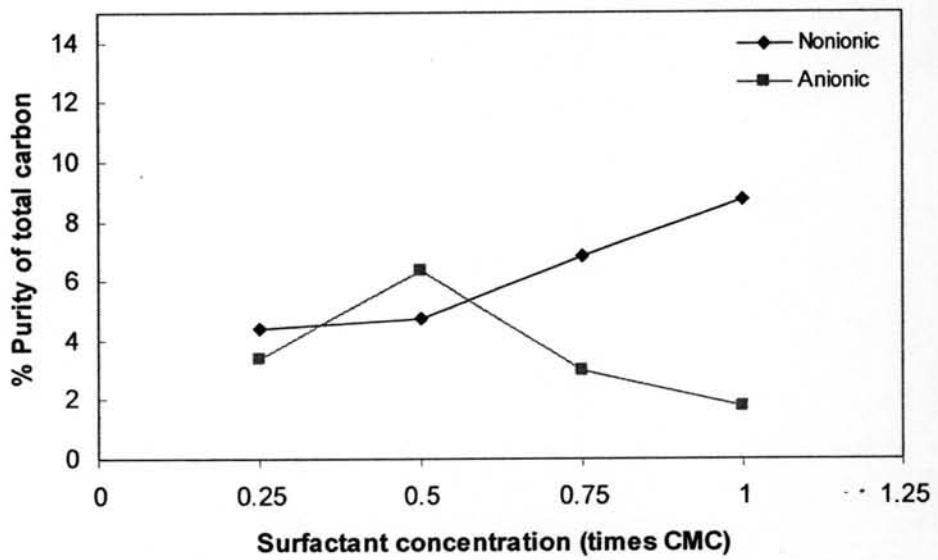

Figure 4.17 Effect of surfactant concentration with anionic or nonionic surfactant after oxidative and acid treatment. The froth flotation experiment were operated at air flow rate at 170 ml/min and pH 5.

Figure 4.17 illustrates the purity of SWNTs using temperature programed oxidation (TPO) to evaluate the quantitative purity of SWNTs of the froth flotation step, by comparing two types of surfactants: sodium dodecyl benzene sulfonate (SDBS: anionic) and alcohol ethoxylate surfonic L24-7: nonionic. As shown in Figure 4.17, the carbon purity increases slightly with increasing nonionic surfactant concentration but the carbon purity changed insignificantly. The results suggest that the froth flotation step used in this study cannot improve the carbon purity. Figure

4.18 shows the SWNT bundles still attach firmly with silica surface. Hence, the pretreatment steps of the air oxidation and acid treatment could not separate the SWNTs form the silica. Therefore, NaOH was used to dissolve the silica before running the froth flotation experiment.

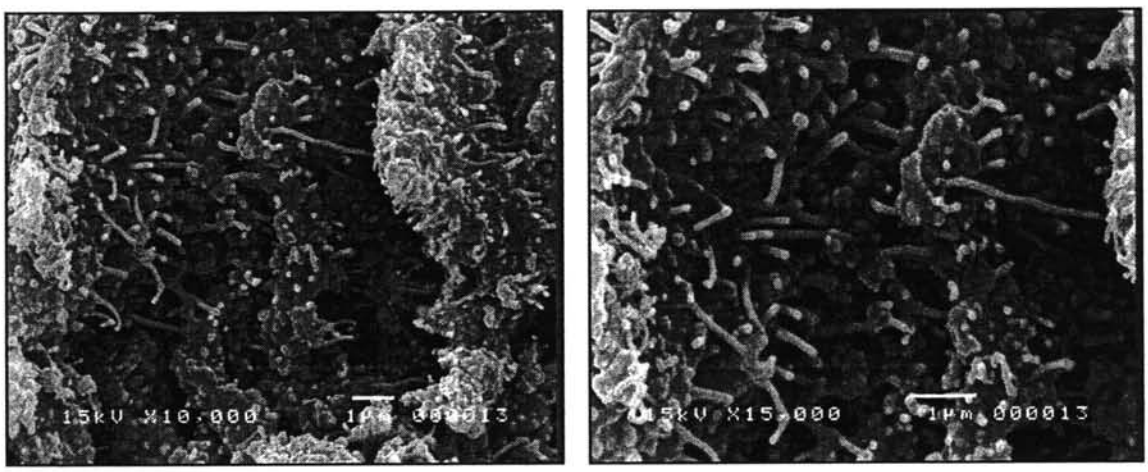

(a) (b)

Figure 4.18 Scanning electron microscope (SEM) images of SWNT samples of froth flotaion after acid treatment: (a) 10000 x, and (b) 15000 x.

For the silica dissolution study, 0.01 g of the SWNT sample after the air oxidation and acid treatments was further treated with 1.5 ml of 5 M sodium hydroxide solution at 70°C for 12h. These optimum conditions used were adopted from previous studies (Kiatsoongchart., 2005 and Chuaybumrung., 2006)

Table 4.10 Comparison of silica removal of fresh catalyst, as-prepared SWNTs, and pretreated SWNTs using 5 M NaOH at 70°C and 12 h

Types	% Removal
Fresh catalyst	93.1
As-prepared SWNTs	58.4
Pretreated SWNTs	62.6

Table 4.10 and Figure 4.19 summarize the percentage of silica removal the pretreated SWNTs as compared to the fresh catalyst and the as-pretreated SWNTs. The results show that for the fresh catalyst sample almost complete silica removal upto 93% was achieved by dissolving with 5 M NaOH solution at 70°C and 12 h. However, for both as-prepared SWNTs and pretreated SWNTs, the silica removal was very low about 58.4 and 67.6%, respectively. The results of the low silica removal of the as-prepared SWNT sample can be explained in that the surface of silica is partially covered by the SWNT bundles. From the results also suggest that the pretreatment step of air oxidation and acid treatment can not increase the exposure surface of the silica.

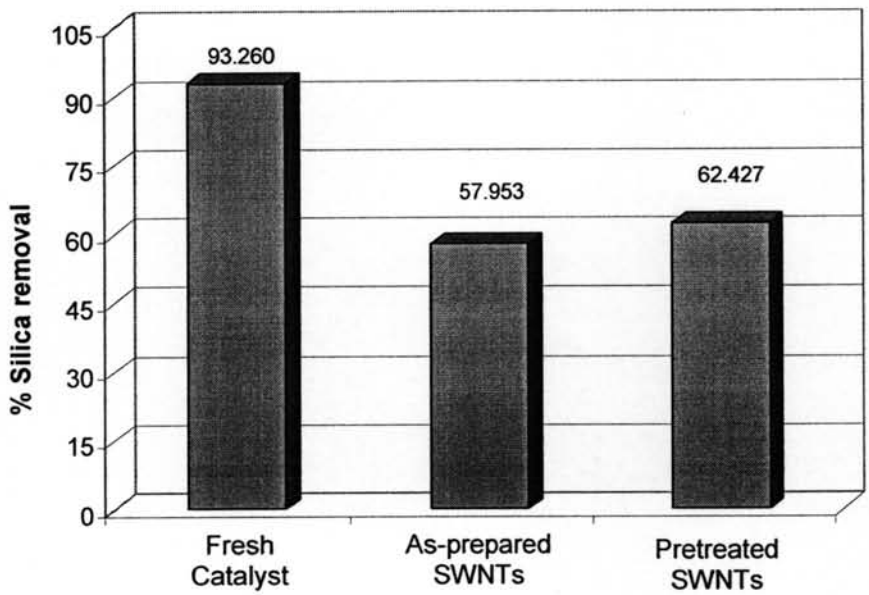

Figure 4.19 Comparison of silica removal of fresh catalyst, as-prepared SWNTs, and pretreated SWNT samples using 5 M NaOH, 70°C and 12 h.

4.8. Froth Flotation Results

In this froth flotation study, the SWNT sample was pretreated with three sequential steps of air oxidation, HCl leaching and NaOH treatment under the optimum conditions as mentioned before. Two types of surfactants; SDBS and Surfonic L24-7 were used as frothers.

4.8.1 Pure surfactant system

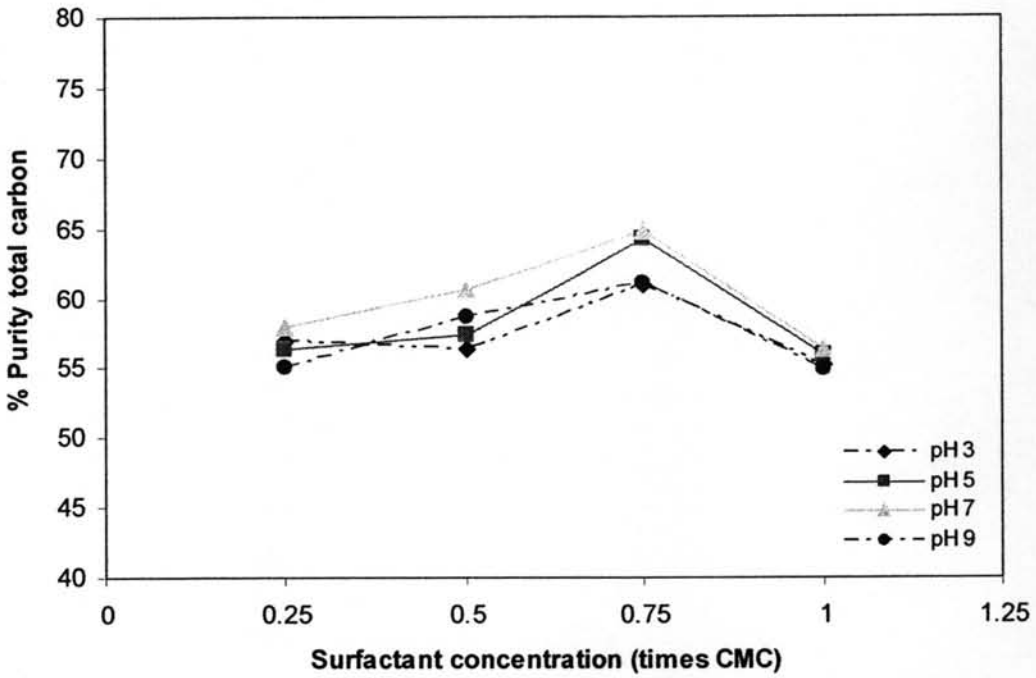

Figure 4.20 Effect of nonionic surfactant concentration with varying pH solutions on the carbon purity of froth flotation operated at an air flow rate of 170 mL/min.

From the results as shown in Figure 4.20, for any given solution pH, the purity of the SWNTs increases with increasing nonionic surfactant concentration upto 0.75 times the CMC as a consequence of the greater amount of surfactant creating more a hydrophobic region. This region is available for SWNT particles to attach into froth flotation zone. Matarredona. *et al.,* (2003) reveal that the nanotubes walls are mostly hydrophobic in nature and so an increase in surfactant concentration results in increasing the separation efficiency of SWNTs. However, beyond 0.75 times CMC, the purity of SWNTs decreased with increasing surfactant concentration due to the high adsorption of surfactant onto the air bubble surfaces, which may hold both SWNT and silica particles on the top of the froth flotation column. For the case of SDBS anionic surfactant, the carbon purity has a similar trend as increased and then decrease, as shown in Figure 4.21. For both types of studied surfactants, the effect of solution pH on the carbon purity was found to be insignificant in the studied conditions.

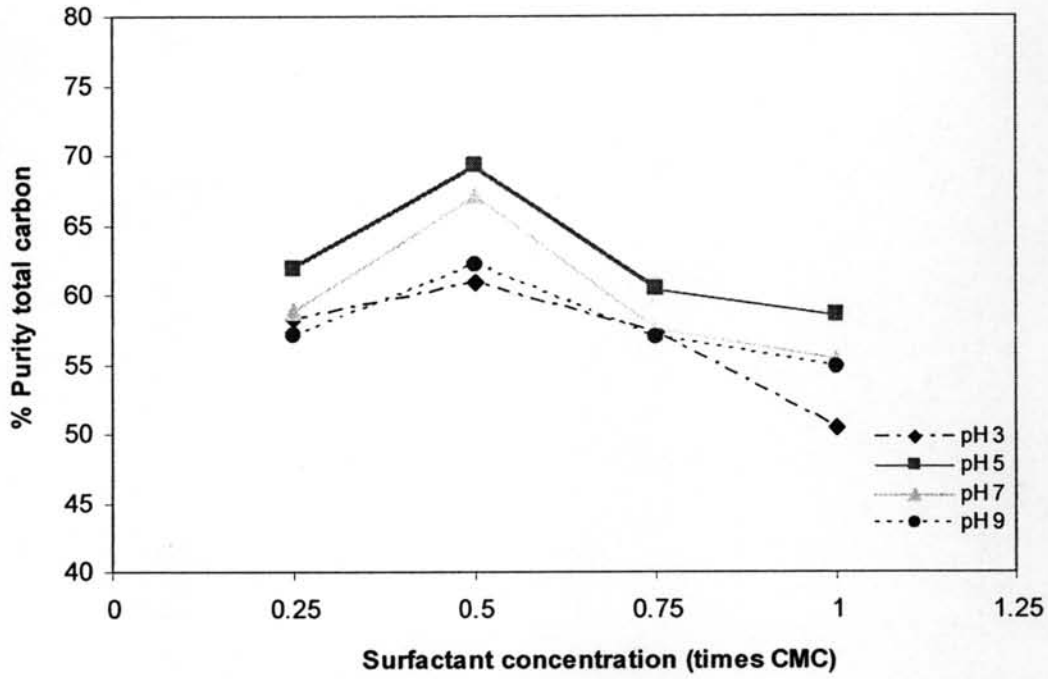

Figure 4.21 Effect of anionic surfactant concentration with solutions of varying pH at170 ml/min after acid treatment and silica dissolution.

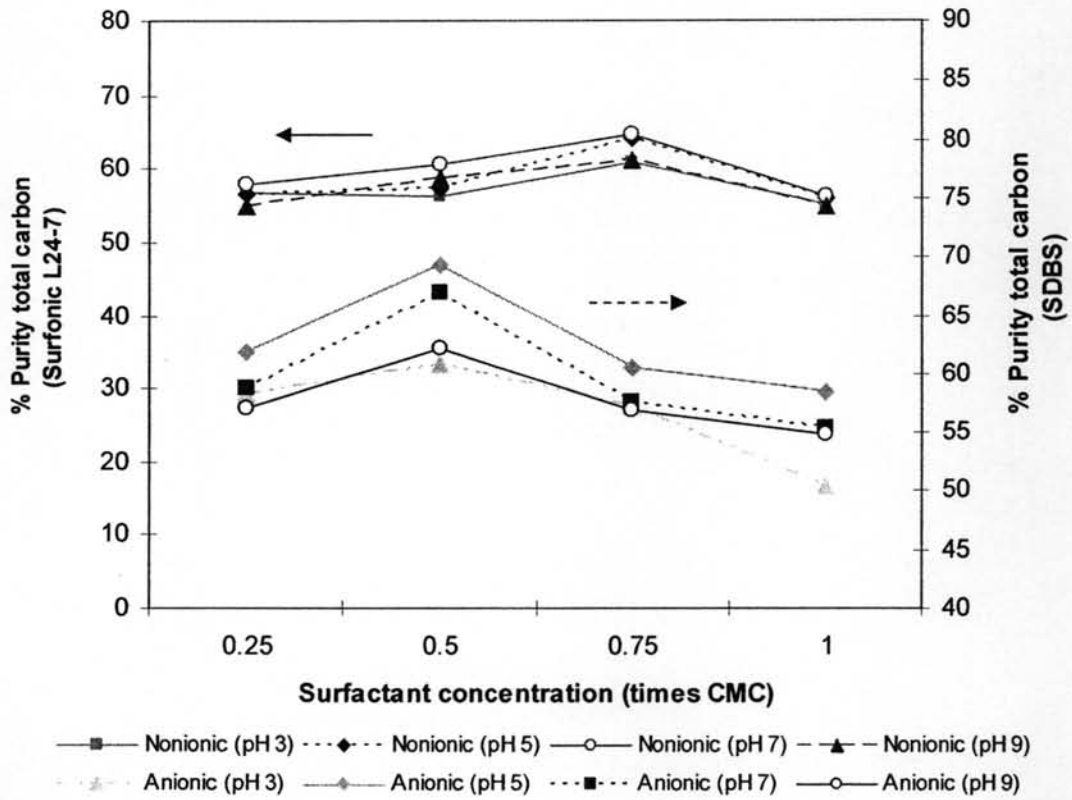

Figure 4.22 Effect of surfactant types with different concentrations at 170 ml/min after acid pretreatment and silica dissolution.

Figure 4.22 shows the similar performance of froth flotation in carbon separation using the two studied surfactants. Hence, mixed surfactants were further studied in order to improve the separation efficiency of froth flotation.

4.8.2 Comparisons of Pure and Mixed Surfactant systems

To compare four types of nonionic, anionic, and a mix of nonionic sand anionic surfactant at the ratio 1:12, and 1:1 to determine one provides superior performance for distinguishing between silica and SWNTs, the percent purity of the SWNTs was investigated.

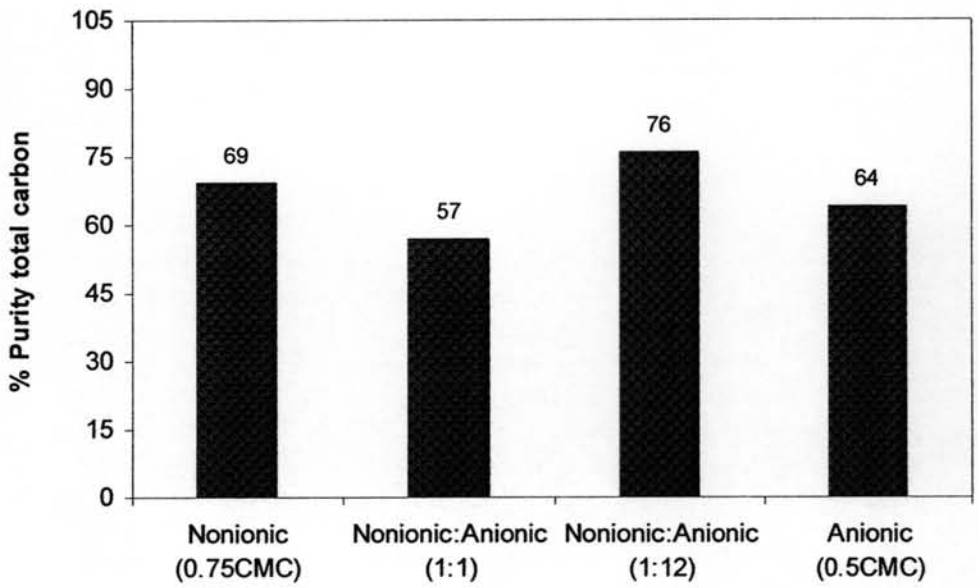

Figure 4.23 Comparison of mixed surfactants and anionic surfactant at 170 ml/min at pH 5 after acid treatment and silica dissolution.

Figure 4.23 exhibits that the percent purity of mixed surfactant at (1:12.24) of nonionic: anionic surfactant is highly effective for separation and obtained the highest purity at approximately 75.96% as a consequence of the synergistic effects (Harwell. *et al.,* 2005). This is due to nonionic surfactant reduces

repulsion of the head group and creates a more hydrophobic region than pure anionic surfactant. However, the excess of nonionic surfactant in the mixture of (1:1) nonionic: anionic surfactant dramatically provided lower purity as a resulting of excess of nonionic surfactant having a highly hydrophobic region, which can hold silica particle into the froth flotation.

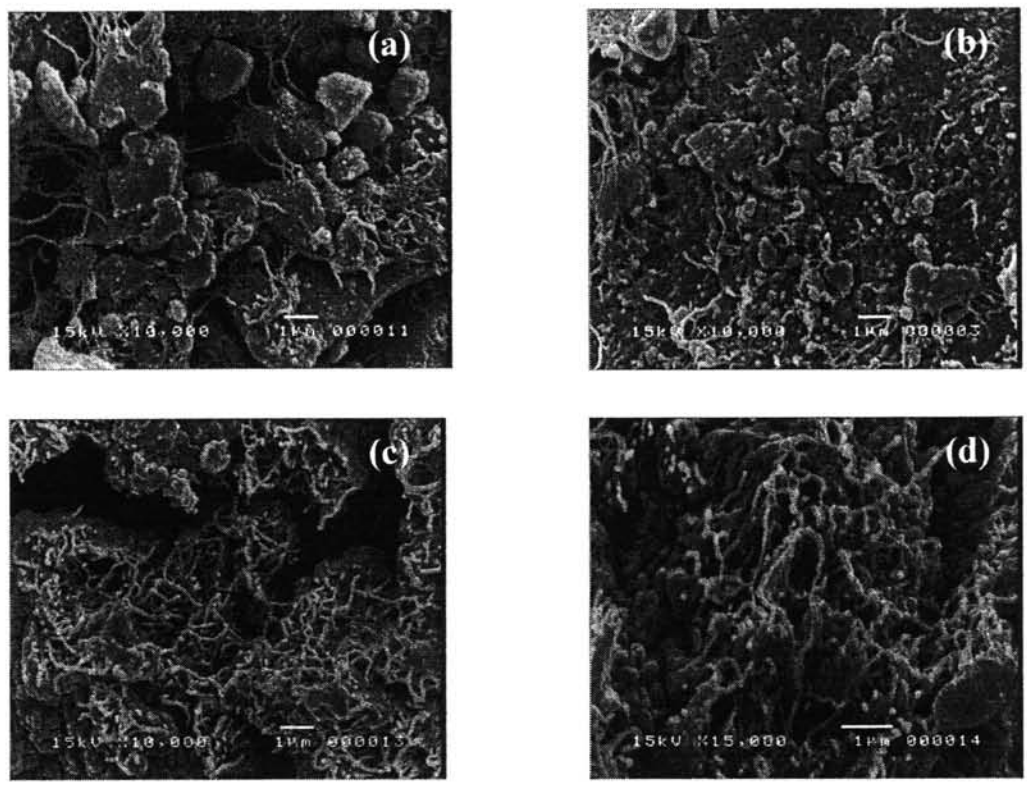

Figure 4.24 Scanning electron microscope (SEM) images of as-prepared SWNTs (a) as-prepared SWNTs, (b) after oxidative and acid treatment, (c) after silica dissolution, (d) after froth flotaion.

Figure 4.24 shows SEM images of SWNTs after each sequential step. The SEM image of as-prepared SWNTs highly contains a large fraction of impurities in their SWNTs at approximately 97.5% as shown in Figure 4.24 (a). The SWNTs purity was increased at about 3.67% with further treated with oxidative pretreatment and acid treatment. For silica dissolution, the SWNTs purity was further improved up to 35% by using NaOH. After froth flotation step, the SWNTs purity was improved to 71% as compared to 2.55% of original total carbon purity of as-prepared SWNTs. This is

because the surfactant creates hydrophobic region and forms micelle in which is available for SWNTs attachment in this region.